Cell Biol Toxicol (2014) 30:1–16
DOI 10.1007/s10565-013-9265-y

ORIGINAL RESEARCH

Nano-sized and micro-sized polystyrene particles affect phagocyte function

B. Prietl · C. Meindl · E. Roblegg · T. R. Pieber · G. Lanzer · E. Fröhlich

Received: 3 September 2013 / Accepted: 15 November 2013 / Published online: 29 November 2013

Abstract Adverse effect of nanoparticles may include impairment of phagocyte function. To identify the effect of nanoparticle size on uptake, cytotoxicity, chemotaxis, cytokine secretion, phagocytosis, oxidative burst, nitric oxide production and myeloperoxidase release, leukocytes isolated from human peripheral blood, monocytes and macrophages were studied. Carboxyl polystyrene (CPS) particles in sizes between 20 and 1,000 nm served as model particles. Twenty nanometers CPS particles were taken up passively, while larger CPS particles entered cells actively and passively. Twenty nanometers CPS were cytotoxic to all phagocytes, ≥500 nm CPS particles only to macrophages. Twenty nanometers CPS particles stimulated IL-8 secretion in human monocytes and induced oxidative burst in monocytes. Five hundred nanometers and 1,000 nm CPS particles stimulated IL-6 and IL-8 secretion in monocytes and macrophages, chemotaxis towards a chemotactic stimulus of monocytes and phagocytosis of bacteria by macrophages and provoked an oxidative burst of granulocytes. At very high concentrations, CPS particles of 20 and 500 nm stimulated myeloperoxidase release of granulocytes and nitric oxide generation in macrophages. Cytotoxic effect could contribute to some of the observed effects. In the absence of cytotoxicity, 500 and 1,000 nm CPS particles appear to influence phagocyte function to a greater extent than particles in other sizes.

Keywords Cytotoxicity · Nanoparticle · Phagocytosis · Interleukins · Inflammation · Oxidative burst

Electronic supplementary material The online version of this article (doi:10.1007/s10565-013-9265-y) contains supplementary material, which is available to authorized users.

B. Prietl · T. R. Pieber · E. Fröhlich
Department of Internal Medicine, Division of Endocrinology and Metabolism, Medical University of Graz, Auenbruggerplatz 15, 8036 Graz, Austria

C. Meindl · E. Fröhlich (✉)
Center for Medical Research, Medical University of Graz, Stiftingtalstr. 24, 8010 Graz, Austria
e-mail: eleonore.froehlich@medunigraz.at

E. Roblegg
Institute of Pharmaceutical Sciences, Department of Pharmaceutical Technology, Karl-Franzens-University of Graz, Humboldtstr, 46, 8010 Graz, Austria

G. Lanzer
Department of Blood Group Serology and Transfusion Medicine, Medical University Graz, Auenbruggerplatz 3, 8036 Graz, Austria

Introduction

Nanoparticles (NPs) are increasingly finding applications in medicine; for example, in diagnostic devices, drug targeting, cell tracking and regenerative medicine. Potential adverse effect of NPs may include interference with the immune system.

The immune system consists of cellular and humoral elements and can be classified into specific (adaptive, acquired) and unspecific (innate) responses. The effector cells for the adaptive immune system are B- and T-lymphocytes. Innate immunity consists of anatomical barriers, phagocytic cells in the blood (monocytes, granulocytes) and in the tissues (macrophages), and

various humoral factors, such as coagulation system, complement system, lactoferrin, transferrin, lysozyme and interleukin 1, in the blood. Monocytes, macrophages and dendritic cells, in addition to unspecific phagocytosis, are linked to the specific immune system and display a variety of physiological reactions. Main functions include migration to a chemotactic stimulus (chemotaxis), secretion of cytokines, phagocytosis, processing and presentation of antigens and bactericide reactions (nitric oxide generation, oxidative burst, myeloperoxidase release etc.).

Existing size-dependent in vivo studies in rodents mainly focussed on the respiratory tract and investigated a panel of different materials. These data show stronger stimulation of the immune system by 14 nm carbon black particles than by 95 nm particles (Shwe et al. 2005). Polystyrene latex particles of 25 and 50 nm had a stronger effect than 100 nm particles (Inoue et al. 2009), while 50 and 200 nm gold NPs caused similarly little inflammation (Gosens et al. 2010). These data suggest stronger immune stimulation by smaller than by larger particles.

In vitro studies on biodegradable and non-biodegradable NPs show that these particles can interfere with a variety of phagocyte functions. In these studies, mostly either nano- or micro-sized particles were studied, which prevents conclusions on size-dependent effects.

Non-biodegradable gold (Villiers et al. 2010), amorphous silica (Winter et al. 2011), silver (Yang et al. 2012), TiO_2 (Liu et al. 2010), and ZnO (Heng et al. 2011) NPs, but also biodegradable NPs, such as poly(lactic-*co*-glycolic acid) (Segat et al. 2011), chitosan (Yue et al. 2010) and hydroxyl apatite (Scheel et al. 2009) induce secretion of inflammatory cytokines by phagocytes.

Pegylated gold, silica and TiO_2 NPs (Park and Park 2009; Hutter et al. 2010; Scherbart et al. 2011) increased nitric oxide production, whereas silver and CeO_2 NPs (Hirst et al. 2009; Shavandi et al. 2011) decreased nitric oxide production. Carbon nanotubes, TiO_2 NPs and Al NPs reduced phagocytosis (Hsiao et al. 2008; Witasp et al. 2009; Liu et al. 2010), and carbon nanotubes, polymethylmethacrylate NPs and TiO_2 NPs suppressed chemotaxis (Papatheofanis and Barmada 1991; Witasp et al. 2009; Liu et al. 2010). TiO_2, Ti, V and polylactic acid particles of 266 to 3,000 nm induced superoxide production in granulocytes (Hedenborg 1988; Kumazawa et al. 2002; Mainardes et al. 2009). Fullerenes inhibited the degranulation of granulocytes, while TiO_2 NPs had no effect (Jovanovic et al. 2011; Vesnina et al. 2011).

The fact, that similar effects on phagocytes were caused by quite different types of NPs, favours the idea that this phenomenon could be studied using model particles.

Carboxylated polystyrene (CPS) particles are used for cellular tracing and studies of size-dependent NP effects since they lack (heavy metal) contamination, do not interfere with screening assays, and show only minimal production of reactive oxygen species (Fröhlich et al. 2009). Also, they are available with physically trapped fluorochrome, allowing the localisation of the particles in cells and tissues (Fröhlich et al. 2012a; Roblegg et al. 2012; Fröhlich et al. 2013). Particle uptake, cytokine secretion, phagocytosis, nitric oxide generation, superoxide production and myeloperoxidase release served as parameters for phagocyte function. Cytotoxicity of variable sized CPS particles in differentiated and non-differentiated monocytes was compared to test the hypothesis that cytotoxicity may be caused in part by generation of reactive oxygen species accompanying phagocytosis (Olivier et al. 2003). Although particle shape plays an important role in the interaction of NPs with phagocytes (Champion and Mitragotri 2009), only spherical particles were investigated. The investigation aims to identify the effect of particle size on cytotoxicity and on different phagocyte functions. To this aim, various cell types had to be used because not all phagocytes are suitable for the assessment of specific phagocyte functions.

Materials and methods

Particles

Carboxyl polystyrene latex beads (20,100, 200, 500 and 1,000 nm), and their respective fluorescent beads, where dye is physically trapped inside the particle (red FluoSpheres®) were obtained from Invitrogen. In the fluorescent particles, the dye is integrated in the core, which has the advantage that fluorescent and non-fluorescent particles have the same surface properties. CPS suspensions were put into an Elmasonic S40 water bath (ultrasonic frequency, 37 kHz, 40 W, Elma) for 20 min prior to cell exposure and for physicochemical characterisation.

Particles were applied plasma-coated and uncoated in PBS (myeloperoxidase, superoxide formation and chemotaxis) and without plasma coating in DMEM (cellular uptake, cytotoxicity, nitric oxide generation, phagocytosis and cytokine secretion).

Isolation of peripheral blood monocytic cells

Peripheral blood monocytic cells (PBMC) were isolated from buffy coat residues obtained from the University Clinic of Blood Group Serology and Transfusion Medicine after informed consent from the patients. The buffy coat residue (9 ml) was diluted in sterile phosphate-buffered saline (PBS; 15 ml). The resulting suspension (8 ml) was layered on Histopaque 1077 HybriMax solution (3 ml; Sigma). After centrifugation at 400×*g* for 30 min at RT the cell layer was collected, washed with Hepes-buffered salt solution (Invitrogen) and centrifuged again 3×10 min at 250×*g*. The pellet was resuspended in 5 ml RPMI medium+10 % foetal bovine serum (FBS); 5 ml) and cells were counted in a Coulter Counter AcT diff AL (Beckmann Coulter Inc).

Cell lines

THP-1 human acute monocytic leukaemia cells (Cell Line Services), DMBM-2 murine macrophages and U937 human histocytic lymphoma cells (Deutsche Sammlung für Mikroorganismen und Zellkulturen) were cultured in the medium recommended by the producer.

Differentiation of monocytes

THP-1 cells were differentiated into macrophages by exposure to phorbol 12-myristate 13-acetate (PMA; 1 ng/ml; Sigma) for 48 h in RPMI+10 % FBS prior to exposure to the lipopolysaccharide (LPS) positive control (100 ng/ml; Sigma) and to the particle suspensions for 24 h. For U937 cells, differentiation by exposure to PMA (10 ng/ml) for 24 h was used. The optimum concentration and duration of the treatment was identified by observation of morphological changes (increase in cell size and adhesion to the culture well) that indicate the differentiation into macrophages.

Physicochemical characterisation

Particles were characterised in terms of size and zeta potential by photon correlation spectroscopy and laser Doppler velocimetry (scattering angle of 17°) using a ZetaSizer Nano-ZS (Malvern Instruments, UK). Particles were diluted in the solvents to a concentration of 200 μg/ml. After equilibration of the sample solution to 25 °C, hydrodynamic sizes were measured with a 532-nm laser and a detection angle of 173°. Dynamic fluctuations of light scattering intensity caused by Brownian motion of the particles were evaluated. The zeta potential was measured by laser Doppler velocimetry (scattering angle of 17°) coupled with photon correlation spectroscopy (Zetasizer Nano ZS, Malvern Instruments, Malvern, UK) and calculated out of the electrophoretic mobility by applying the Henry equation.

Quantification of endotoxin

PYROGENT Ultra (sensitivity=0.06 EU/ml, Lonza) was used for the endotoxin testing. Each sample dilution was tested in duplicate, and the different endotoxin standards with *Escherichia coli* strain 055:B5 in triplicates. The assay was performed first as a yes/no test and samples with positive endotoxin detection were further tested via a dilution series to quantify free endotoxin. The assay was performed according to the instructions given in the manual.

Determination of cellular dose

DMBM-2 cells (adherent) and THP-1 monocytes (suspension) were exposed to 20 μg/ml of red FluoSpheres® in DMEM for 24 h. Medium height was 3 mm. DMBM-2 cells were washed three times with medium, removed from the plastic support by trypsin treatment and resuspended in medium. THP-1 cells were collected and washed by centrifugation. Fluorescence of the cells and of serial dilutions of the exposure solution was measured on a fluorescence plate reader (FLUOstar Optima, BMG Labortechnik) at 584/612 nm. The exposure solution was diluted with cell suspensions instead of medium alone to account for autofluorescence or quenching effects caused by the cells. Cell numbers/well were determined using CASY® Cell Counter+Analyser System Model TT (Roche Innovatis).

Cytotoxicity screening (formazan bioreduction)

Formazan bioreduction by cellular dehydrogenases was assessed using the CellTiter 96® AQueous Non-Radioactive Cell Proliferation Assay (Promega) after 4 and 24 h of exposure to CPS according to the manufacturer's instructions and absorbance was read at 450 nm on a SPECTRA MAX plus 384 (Molecular Devices). To identify potential interference with the assay, appropriate controls (particles+assay compounds and particles+cells) were included.

To correlate cytotoxicity to particle number/cell, % uptake as determined with FluoSpheres® was expressed as particle numbers (according to data sheet provided by the producer) and divided by the number of seeded cells.

Cytotoxicity screening (quantification of ATP)

ATP detection in healthy mitochondria is based on the ATP-dependent luminescence by luciferase. The CellTiter-Glo luminescent cell viability assay (Promega) was used according to the manufacturer's instructions and luminescence was read on a Lumistar (BMG Labortechnik). To identify potential interference with the assay, appropriate controls (particles+assay compounds and particles+cells) were included.

Intracellular localisation of particles

PBMCs were incubated with red FluoSpheres® (25 μg/ml in DMEM) for 30 min and 24 h. To differentiate between active and passive processes, incubations for 30 min were performed at 37 and at 4 °C, respectively. Granulocytes were isolated from human fresh whole blood by the use of a 3 % dextran/NaCl solution. Alternatively, DMBM-2 cells were incubated with red FluoSpheres® (40 μg/ml) suspended for 3 h in the presence of cytochalasin B (10 μM; Sigma) or sodium azide (1 mM).

After the incubations with the particles, cells were washed in PBS, fixed with *p*-formaldehyde (4 %) for 10 min at RT and rinsed three times in PBS. Aliquots of PBMC samples stained with FITC-labelled anti-CD3 (anti-human, 5 μl, BD), FITC-labelled anti-CD13 antibody (anti-human, 5 μl, BD) and AF488-labelled anti-CD14 (anti human, 5 μl, BD) for 30 min at 37 °C to discriminate between lymphocytes, granulocytes and monocytes and counterstained with Hoechst33342 (1 μg/ml) for 15 min at RT. DMBM-2 cells were stained with HCS CellMask blue (2 μg/ml, Invitrogen) for 30 min. Extracellular fluorescence and quenched by the addition of Trypan blue (0.25 mg/ml). Cells were viewed with a LSM510 Meta confocal laser scanning microscope (Zeiss).

Chemotaxis assay

U937 cells were cultured in "starving medium" (RPMI-1640 medium with 0.2 % BSA, 1.5 g/l sodium bicarbonate, 4 mM L-glutamine, 100 U/ml penicillin and 100 μg/ml streptomycin sulphate) for 24 h. For testing, the cells were put into transwells with 3-μm filters (Multiscreen Filtration System, Millipore) and exposed to control chemoattractant (medium with 20 % plasma), negative control (PBS for uncoated CPS particles, and plasma diluted 1:30 in medium for plasma-coated CPS particles) and medium (background) for 4 h. CPS particles were coated with human plasma (one part fresh frozen plasma and 29 parts CPS particles) for 60 min at RT. In a further set of experiments, U937 cells were pre-incubated with CPS particles for 30 min and, subsequently, exposed to 50 ng/ml PMA as chemoattractant. Cell migration through the filter was quantified using the ATP-content assay (see cytotoxicity screening).

Quantification of interleukin-6 and interleukin-8 release

Supernatants of the cells exposed to 10, 20 and 50 μg/ml CPS particles suspended in DMEM for 24 h or to medium without particles were assessed. The release of IL-6 and IL-8 was measured using the human IL-6 ELISA set (BD OptEIA™) and the human IL-8 ELISA set (BD OptEIA™, BD Biosciences) according to the protocol given by the producers. Absorbance was read at 450 nm on a SPECTRA MAX plus 384 photometer.

Phagocytosis

The Vybrant phagocytosis assay (Invitrogen) uses the amount of ingested fluorescent bacteria (*E. coli* K-12 BioParticles) for the assessment of phagocytosis. Medium (50 μl) or CPS suspension in medium was added to a suspension of DMBM-2 mouse macrophages (10^5/100 μl) and the mixture incubated for 1.5 h at 37 °C. Subsequently, the FITC-labelled *E. coli* suspension was added and incubated for 2 h at 37 °C, the extracellular fluorescence quenched by the addition of Trypan blue

(0.25 mg/ml), and the uptake measured on a FLUOstar Optima (ex 480 nm/em 520 nm).

Superoxide formation

The Phagoburst™ assay (Immunodiagnostics) quantifies the leukocyte oxidative burst in human whole blood samples and was performed according to the instructions given by the producer. Upon incubation with the positive control (*E. coli*) or CPS particles, induction of reactive oxidants is monitored by the addition and oxidation of dihydrorhodamine 123. The kit was used according to the instructions in the manual. Plasma-coated and uncoated CPS particles were incubated with heparinised whole blood samples from healthy human individuals for 10 min at 37 °C. PMA (8.1 μM) and plasma (1:30 in PBS) without particles served as positive and negative controls, respectively. Cells were analysed with a FACSCanto II cytometer (BD Biosciences) and BD FACSDiva™ software.

Quantification of nitric oxide

Nitrite (NO_2^-) is the stable product of the antimicrobial effector molecule nitric oxide (NO). Thus, to measure nitric oxide production in the mouse macrophage DMBM-2 cells Griess reagent was used, which detects nitrite. This reagent was obtained by addition of equal amounts of 1 % sulphanilamide in 5 % phosphoric acid and 0.1 % *N*-(1-naphthyl) ethylenediamine dihydrochloride in water. DMBM-2 cells were cultured in phenol-free RPMI-1640 medium for 24 h and treated with CPS particles suspended in medium for a further 48 h. In a fresh 96-well plate, the supernatant (50 μl) was added to the Griess reagent (100 μl). After incubation for 10 min in the dark, absorbance at 520 nm was determined using a SPECTRA MAX plus 384 photometer.

Quantification of myeloperoxidase

Blood from healthy volunteers (after informed consent) was collected by venipuncture and collected in lithium heparin tubes. An equal volume of CPS particles suspended in PBS and blood was mixed and incubated for 1 h in the dark; PMA (100 nM; Sigma) served as positive control. Samples were centrifuged to remove platelets, initially for 15 min at 1,000×*g* at 4 °C and subsequently for 10 min at 10,000 g. MPO activity was quantified in the diluted supernatant (1:20–1:50) using a human MPO ELISA kit (Hoelzel Diagnostics) and absorbance was measured at 450 nm on a SPECTRA MAX plus 384 photometer. In parallel to the quantification of MPO, lactate dehydrogenase activity was measured in the supernatant to exclude cytotoxicity by using the CytoTox-ONE™ homogeneous membrane integrity assay (Promega). Fluorescence was recorded on a FLUOstar Optima (ex 560 nm/em 590 nm). After subtraction of the blank value the average fluorescence from the samples was normalised to the LDH release of the solvent-treated controls.

Statistical analysis

Data were subjected to statistical analysis and are represented as means ± SD. Data were analysed with one-way analysis of variance (ANOVA) followed by Tukey-HSD post hoc test for multiple comparisons (SPSS 19 software). Nonparametric data were analysed with ANOVA on Ranks followed by Dunn's post hoc test. For the identification of correlation to particle size, Jonckheere Trend (Jonckheere-Terpstra) Test was used. Results with p values of less than 0.05 were considered to be statistically significant.

Results

Prior to the assessment of activation, particles were physico-chemically characterised, tested for biological and chemical contaminations and cytotoxicity of the particles investigated.

Particle characterisation

Particle sizes and charge densities in water were obtained from the producer and compared to characterisation in the media used for the exposures (Table 1). The small 20 nm CPS particles showed twice the size that was indicated by the producer when suspended in PBS or DMEM, while larger CPS particles showed smaller increases. When plasma-coated, the size of 20, 500 and 1,000 nm CPS was similar to the uncoated particles, while particle sizes of 100 and 200 nm CPS increased. Charge densities indicated by the producer increased markedly from 20 and 100 nm CPS to particles ≥200 nm. The zeta potential of the uncoated large CPS suspended in PBS and DMEM, however, was less negative than that of the small ones. After coating with

plasma this trend was even more pronounced; while 20 nm CPS had a zeta potential of −47.2 mV that of 1,000 nm CPS was −10.8 mV.

The presence of bacterial wall compounds (endotoxin) has to be excluded because it is a strong stimulant of inflammation. In the stem suspension (1 mg/ml) of 100 and 200 nm CPS particles traces of endotoxin were detected, at lower concentrations (0.2 mg/ml) endotoxin levels were below detection threshold (<0.06 EU/ml). According to the producer's information surfactant and other low molecular weight substances, which may impair cell viability, are absent. Nevertheless, the biological effect of the solution, in which the particles were provided, was evaluated for the 500 and 1,000 nm particles (all others were too small to be removed from the solution by centrifugation). This data is not mentioned for each assay because these samples reacted similar to the solvent controls.

Cellular uptake

To link particle uptake to biological effects, the amount of ingested particles was quantified in DMBM-2 cells and THP-1 monocytes. While cells contained roughly similar amounts of all particles in terms of % applied dose and mass, this corresponds to roughly 50,000 times more 20 nm CPS particles than 1,000 nm CPS particles in DMBM-2 cells (Table 2). When plasma-coated CPS particles were tested, this difference was smaller (Factor only ~20,000). Plasma-coating decreased the number of ingested particles per DMBM-2 cell dramatically for 20 nm CPS particles to about 50 % for 20 and 100 nm CPS particles, while only small effects were seen for the larger particles. THP-1 monocytes ingested much lower fractions of CPS than DMBM-2 cells (e.g. 1.5 % compared to 25.5 % of 20 nm CPS particles). Plasma-coated 20 nm CPS particles were also taken up to much lower (three times) degree than uncoated ones, while the effect of plasma-coating on uptake was less pronounced for the larger CPS particles (Table 2s, Supplementary Material).

Cellular uptake was also studied by microscopy to differentiate between active and passive mechanisms. Decrease in viability of peripheral blood monocytic cells after 24 h exposure to 20 nm CPS particles shows high variations (100–500 μg/ml), depending on the donor (data not shown). After incubation with particles for 30 min at 37 °C, lymphocytes (CD3-positive), granulocytes (CD13-positive) and monocytes (CD14-positive) have ingested 20 nm fluorescently labelled CPS particles (Fig. 1). Two hundred nanometers CPS particles show slower uptake and, after 30 min of incubation, were seen only inside monocytes and granulocytes. Incubations at 4 °C showed that 500 nm CPS particles were mainly taken up actively and 20 nm CPS particles passively. Uptake of 200 nm CPS particles was only partly blocked by incubation in the cold (Fig. 1) and after 24 h of incubation, 500 nm fluorescently labelled CPS particles were also seen in lymphocytes (Fig. 1), suggesting that 500 nm CPS particles can also be taken up passively. In another approach, the active uptake inhibitor cytochalasin B was used to differentiate between active and passive uptake. Uptake of 1,000 nm CPS particles by DMBM-2 macrophages was reduced, while no inhibition of the uptake of 20 nm CPS particles was seen, also suggesting mainly passive entry of the small CPS (Fig. 1s, Supplementary Material).

Cytotoxicity

To reveal a potential correlation of cytotoxicity and phagocytic activity, viability after exposure to CPS particles in different sizes was measured. After 4 h of incubation to 200 μg/ml 20 nm CPS viability of differentiated and non-differentiated THP-1 cells, and of U937 cells was significantly decreased to 14±2, 14±5 and 15±2 %, respectively. Murine DMBM-2 macrophages were more resistant to the cytotoxic action of CPS particles than the human monocytic cell lines U937 and THP-1. Only at the highest concentration of 20 nm CPS tested the viability of DMBM-2 cells decreased to 43±10 %. One hundred nanometers CPS decreased viability in no experimental condition and 500 nm CPS caused significant loss of viability at the highest concentration tested (62±9 and 72±7 % in differentiated and non-differentiated THP-1 cells, respectively). A similar pattern was also seen at 24 h of exposure (Fig. 2). In all cells, 20 nm CPS particles, but not 100 nm CPS particles, decreased viability (Fig. 2a). Differentiated THP-1 cells, where monocytes differentiated to macrophages according to microscopic features (larger cells, adherence to the plastic well), showed a significantly lower sensitivity to the action of 20 nm CPS particles at 25 and 50 μg/ml. Conversely, cytotoxicity of 500 and 1,000 nm CPS particles was significantly higher (except for 500 μg/ml) in differentiated than in non-differentiated THP-1 cells (Fig. 2b).

The greater cytotoxicity of 20 nm CPS was due to higher cellular uptake. At similar numbers of ingested

Table 1 Overview of physico-chemical characterisation of the CPS particles (size and surface charge) in water (data given by the producer) and in suspension media used in the assays assessed by photon correlation spectroscopy and laser Doppler velocimetry

Particle	Particle size[a] (nm) producer	Size in PBS (nm)	Size in DMEM (nm)	Size (coated) in PBS (nm)	Charge density[a] (μC/cm^2)producer	Zeta pot. in PBS (mV)	Zeta pot. in DMEM (mV)	Zeta pot. (coated) in PBS (mV)
CPS20	26	41	42[b]/300	37.5	0.5	−44.9	−41.2	−47.2
CPS100	140	135	158	247	2.7	−40.0	−36.8	−16.5
CPS200	160	165	230	357	16.8	−35.6	−36.6	−27.6
CPS500	450	563	550	578	14.6	−37.6	−35.7	−20.4
CPS1000	1,100	1,106	1,271	1,494	12.5	−28.8	−29.2	−10.8

PBS phosphate-buffered saline, *DMEM* Dulbecco's modified eagle medium

[a] Data for the lot of CPS particles used for the experiments, provided by the producer

[b] Two peaks of distribution with predominant peak (70 %) indicated first

particles, however, cytotoxicity of 500 nm and 1,000 nm CPS was much higher than that of CPS in smaller sizes (Fig. 3). All cytotoxic effects were more pronounced in THP-1 monocytes (Fig. 3b) than in DMBM-2 macrophages (Fig. 3a): greater decreases in viability were seen at about 100 times lower doses.

Interference with monocyte/macrophage function

Main functions of phagocytes include chemokine-guided extravasation of leukocytes (chemotaxis), secretion of cytokines in monocytes and phagocytosis of pathogens in macrophages.

Chemotaxis, oxidative burst and cytokine secretion

Plasma-coated and non-coated CPS particles of all sizes did not act as chemotactic stimuli for U937 cells (data not shown). Pre-incubation with 1,000 nm CPS particles significantly increased chemotaxis of U937 cells towards PMA as chemoattractant while neither plasma-coated nor uncoated 20 nm CPS particles had a significant effect on chemotaxis (Fig. 4). One thousand nanometers CPS particles reacted significantly different from 20 nm CPS and from 200 nm CPS particles. At 50 μg/ml, also significant differences between 20 and 200 nm CPS particles were noted.

Secretion of the inflammatory cytokines IL-6 and IL-8 was determined upon stimulation with 10–50 μg/ml CPS particles. Similar effects for all concentrations were obtained and effects of exposures to 20 μg/ml are shown. While CPS particles at sizes ≥200 nm appeared to increase the secretion of IL-6 by THP-1 cells, this effect was not significant (Fig. 5a, yellow bars). IL-8 levels were significantly increased upon incubation of THP-1 cells with 20 nm CPS particles (Fig. 5b, yellow bars). After differentiation of THP-1 monocytes with PMA to macrophages 20 μg/ml 500 and 1,000 nm CPS particles significantly increased IL-6 releases (Fig. 5a, red bars). IL-8 secretion was significantly

Table 2 Size-dependent cellular doses in DMBM-2 macrophages

Particles	Uncoated fluorescent CPS				Plasma-coated fluorescent CPS			
	Cellular dose (% applied)	Cellular dose (μg)	Cellular dose (particles)	Particles per cell	Cellular dose (% applied)	Cellular dose (μg)	Cellular dose (particles)	Particles per cell
FS20	25.5±4.0	5.1±0.8	6.6±1.0E+11	1,245,283	17.7±1.3	3.5±0.2	4.6±0.3E+11	730,159
FS100	25.8±3.2	5.2±0.6	7±0.7E+9	12,281	16.4±5.3	3.3±1.1	4.4±0.1E+9	6,286
FS200	18.8±0.2	3.8±0.0	7.3±0.0E+8	1,431	25.7±9.0	5.1±1.8	1.0±0.3E+9	1,538
FS500	25.1±2.2	5.0±0.4	7.7±0.7E+7	148	47.2±7.2	9.5±1.5	1.4±0.2E+8	215
FS1000	40.1±5.6	8.0±1.1	1.1±0.1E+7	22	86.3±4.4	16.3±0.8	2.2±0.1E+7	33

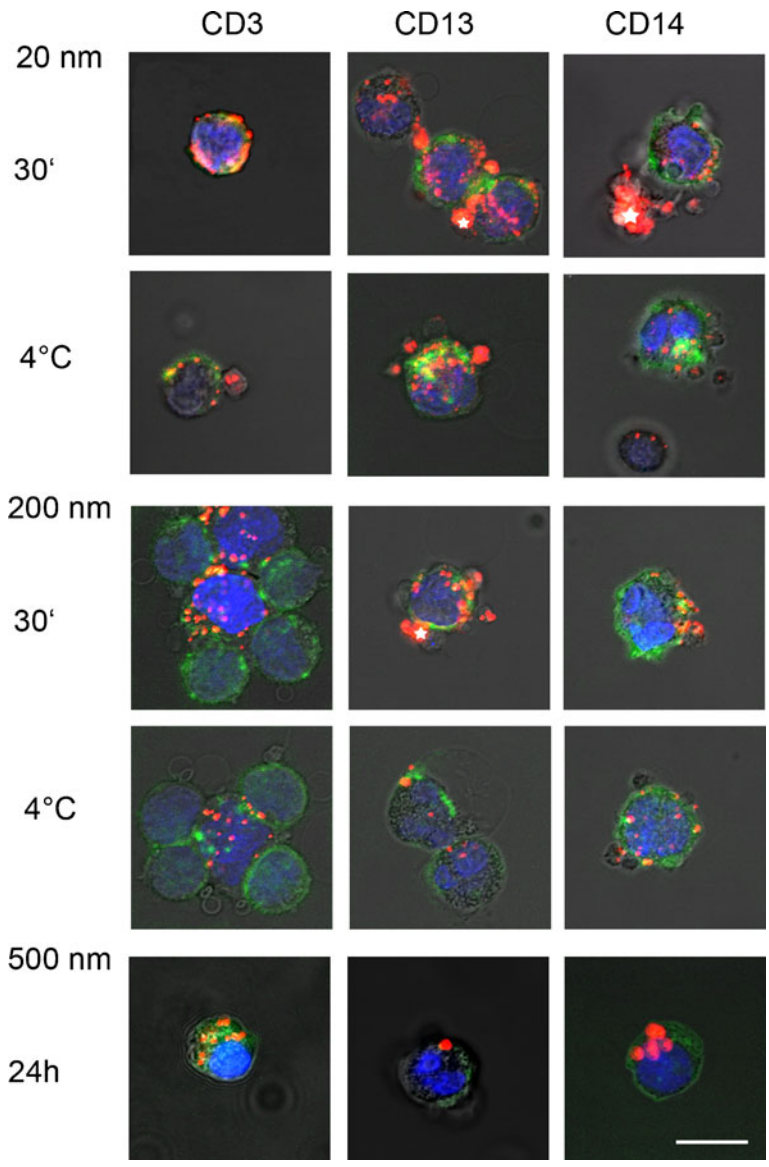

Fig. 1 Uptake of fluorescently labelled carboxyl polystyrene particles (FluoSpheres®, FS) in PBMCs exposed in DMEM. After short incubation at 37 °C, lymphocytes (CD3-immunoreactive) take up 20 nm FS but not larger particles. Granulocytes (CD13-immunoreactive) and monocytes (CD14-immunoreactive) also ingest 200 and 500 nm FS after this time. Uptake of ≥200 nm FS is inhibited by low temperature. After 24 h incubation, lymphocytes also contain 500 nm FS. *Asterisks* indicate FS taken up by platelets. *Scale bar* 10 μm

increased after incubation with CPS particles of 20 and 500 nm (Fig. 5b, red bars). Although relative increases in cytokine secretion induced by CPS particles in non-differentiated and PMA-differentiated monocytes were similar, basal levels of cytokine secretion were higher in the differentiated cells than in the non-differentiated cells. For comparison, basal secretions of 3.0±1.3 pg/ml for IL-6 and 3.5±1.9 pg/ml for IL-8 in non-differentiated THP-1 cells increased to 15.0±4.8 pg/ml for IL-6 and 67.5±10.6 for IL-8 in differentiated cells. A significant correlation of interleukin secretion to CPS particle size is seen for IL-6 secretion in THP-1 monocytes and differentiated THP-1 cells, while IL-8 secretion shows a size-dependent trend only for THP-1 monocytes, not for differentiated THP-1 cells.

In U937 cells CPS particles of all sizes caused only small, insignificant changes of interleukin levels (data not shown). The higher sensitivity of THP-1 cells to particle stimulation relative to that of U937 cells has already been reported (Allermann and Poulsen 2002).

Phagocytosis and nitric oxide generation

DMBM-2 mouse macrophages are used because they present a homogenous population in contrast to monocytes after differentiation with PMA. The phagocytosis

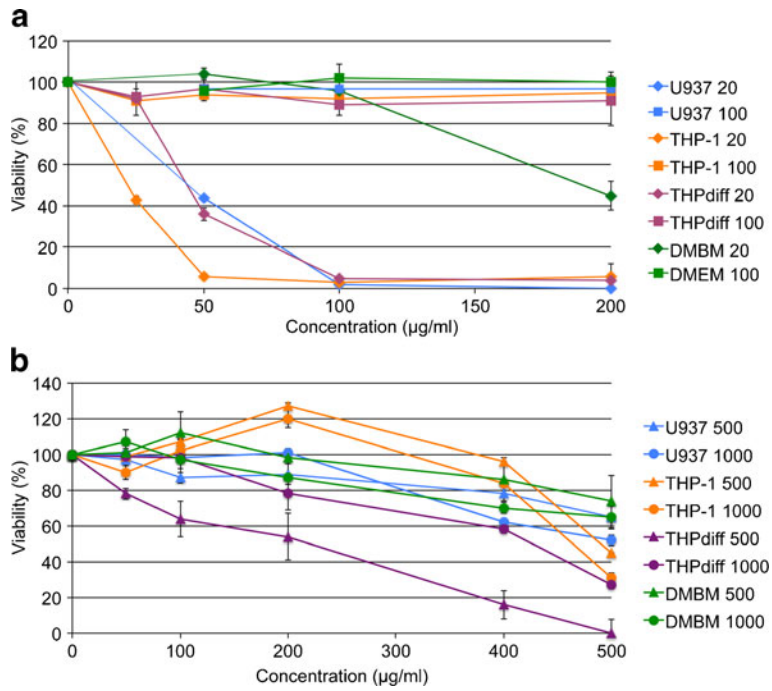

Fig. 2 Viability of human monocytic U937 and THP-1 cells, differentiated THP-1 cells (*THPdiff*) and murine DMBM-2 macrophages after incubation with carboxyl polystyrene particles (CPS particles) of ≤200 nm (**a**) and ≥500 nm (**b**) for 24 h exposed in DMEM (n=4)

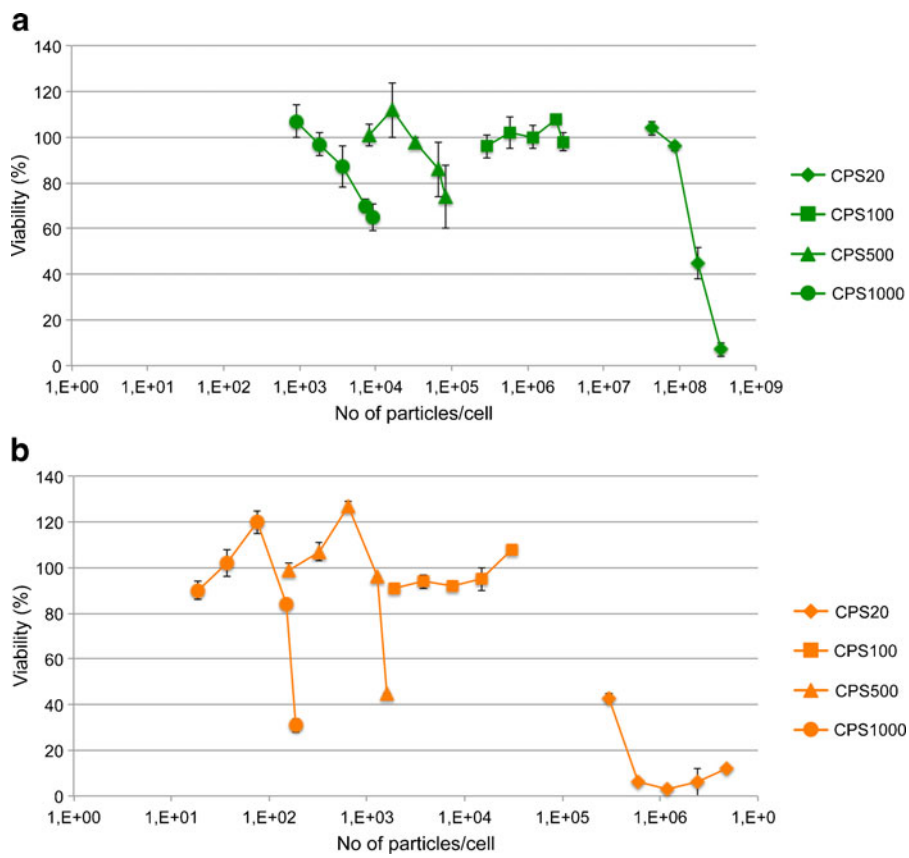

Fig. 3 Viability of DMBM-2 macrophages (**a**) and THP-1 cells (**b**) dependent on particles/cell (n=4). CPS particles decrease viability of monocytic THP-1 cells at lower numbers than viability of DMBM-2 macrophages

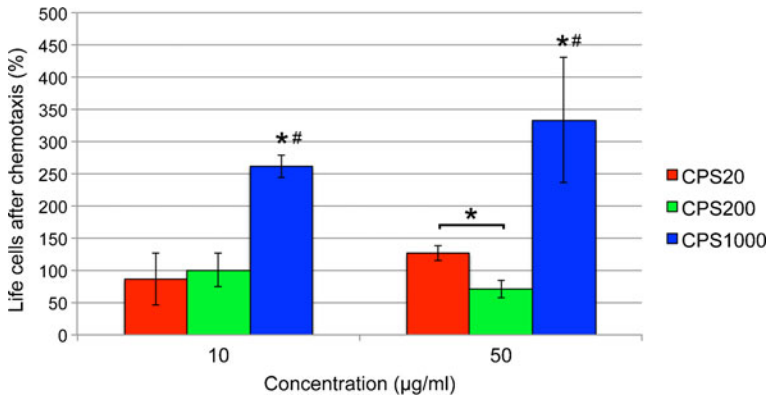

Fig. 4 Chemotaxis of U937 cells towards a positive chemotactic stimulus (PMA) after incubation for 30 min with plasma-coated CPS particles (n=3). Significant changes to the solvent-treated controls (p<0.05) and between different particles linked by brackets are indicated by *asterisk*. A *hatch* indicates significant difference of one particle to the others

of bacteria (*E. coli*, 2×0.5 μm in size) by DMBM-2 cells was completely inhibited at cytotoxic concentrations ≥100 μg/ml 20 nm CPS particles, while non-cytotoxic concentrations inhibited phagocytosis only non-significantly (Fig. 6). Pre-incubation with ≥500 nm CPS particles significantly increased uptake of bacteria.

Concentrations <200 μg/ml did affect nitric oxide generation while most CPS particles in concentrations ≥200 μg/ml and sizes ≥200 nm induced significant increases in nitric oxide generation. Highest nitric oxide production was seen for 500 nm CPS particles. Since effects seen at concentrations of ≥200 μm/ml CPS

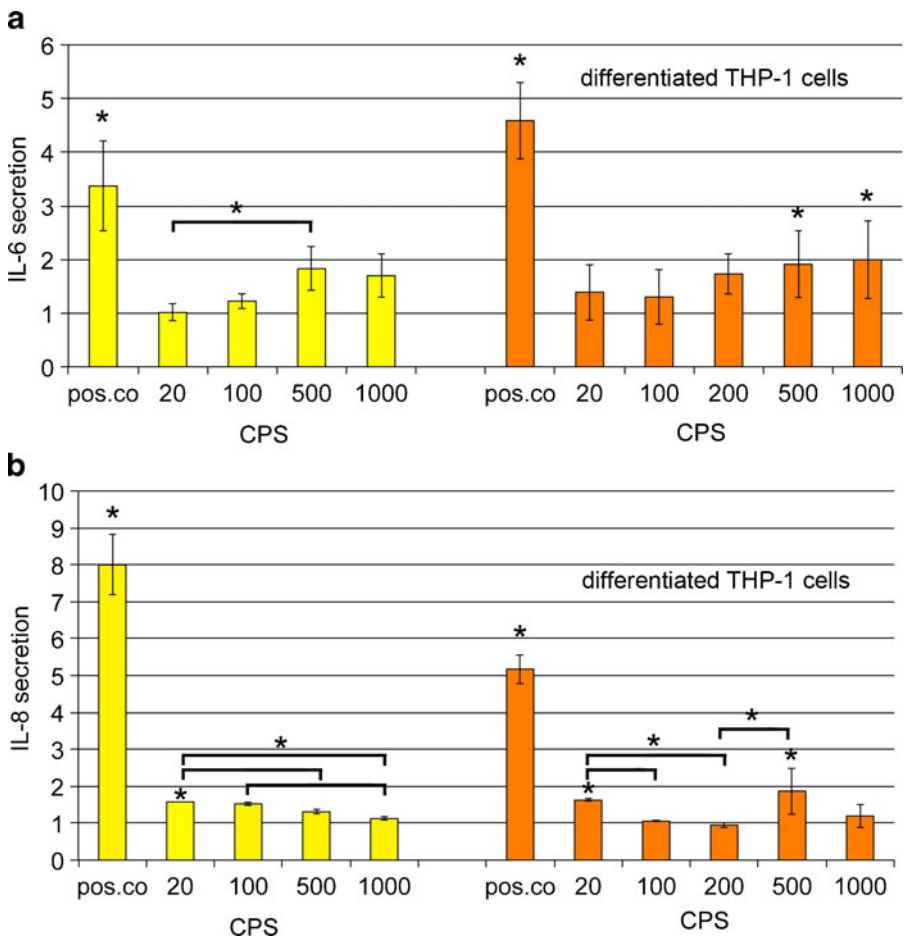

Fig. 5 Release of cytokines IL-6 (**a**) and IL-8 (**b**) from monocytic THP-1 cells upon stimulation with 20 μg/ml CPS particles suspended in DMEM for 24 h (n=6). THP-1 cells were also assessed after differentiation with PMA and releases were normalised to solvent-treated controls as 1. **a** IL-6 secretion was increased by incubations with CPS ≥500 nm. **b** 20 nm CPS stimulated IL-8 secretion in differentiated and monocytic THP-1; 100 ng/ml LPS served as positive control. Significant changes to the solvent-treated controls (p<0.05) and between different particles linked by brackets are indicated by *asterisk*

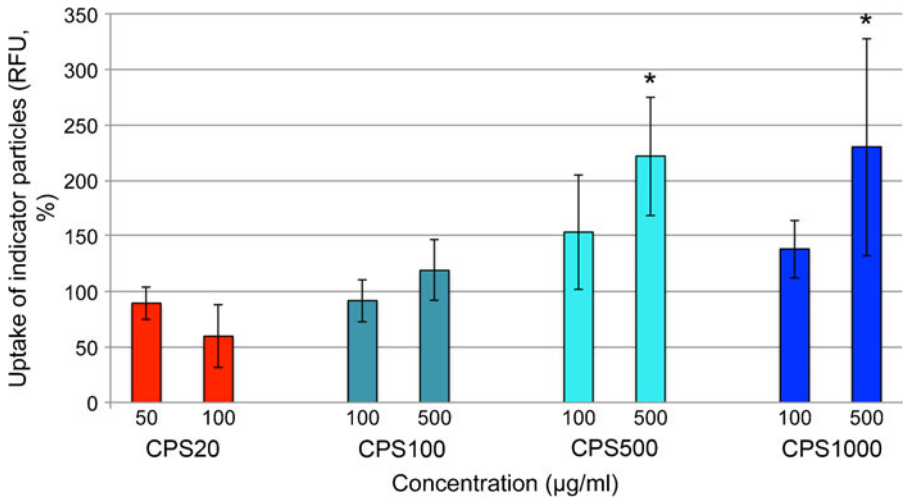

Fig. 6 Phagocytosis of bacteria by DMBM-2 macrophages after pre-incubation with CPS particles suspended in DMEM (n=3). Twenty nanometers CPS particles inhibited phagocytosis, while 1,000 and 500 nm CPS particles stimulated the uptake. Data are normalised (100 %) to the uptake of indicator particles in medium. Significant changes to the solvent-treated controls (p<0.05) are indicated by *asterisk*

particles are not physiologically relevant, data are presented as Supplementary Material (Fig. 2s).

Influence with granulocyte function

Activation of granulocytes can be identified by increase in superoxide production (oxidative burst) and by release of myeloperoxidase. Granulocyte effects can only be detected in primary cells. Since generation of superoxide is also seen in monocytes, both reactions were detected together in blood samples to compare the effect induced by smallest and largest CPS particles.

Effects of 25 μg/ml uncoated and plasma-coated CPS particles were highest for both cell types. Twenty nanometers CPS particles induced generation of superoxide in monocytes of the peripheral blood significantly, while 1,000 nm CPS particles caused no effect (Fig. 7a). Superoxide generation by 20 nm CPS particles was strongly enhanced by coating with plasma. Generation of superoxide by granulocytes was significantly induced by plasma-coated 1,000 nm CPS particles but not by plasma-coated or uncoated 20 and 200 nm CPS particles (Fig. 7b).

Release of myeloperoxidase was assessed up to very high particle concentrations (2 mg/ml) because no effects were seen at lower concentrations. To exclude cytotoxicity at these concentrations, release of LDH was determined in parallel. Myeloperoxidase levels were increased in the supernatant of blood cells after exposure to 20 and 500 nm CPS particles. These (not statistically significant) increases occurred only at high (2 mg/ml) concentrations for 20 nm CPS particles and at 200 μg/ml for 500 nm CPS particles. Since effects at these concentrations are not physiologically relevant, they are supplied as Fig. 3s, Supplementary Material.

An overview on cell types used for the assays, concentrations and sizes of CPS particles, and obtained significant effects, is presented in Table 3.

Discussion

In vitro screening, when possible, prefers cell lines because they usually show smaller inter-assay variations than primary cells. For functional assays, however, the use of cell lines is not always possible because cells tend to lose physiological functions during immortalisation. Functional assays for immune functions often require either primary cells or specific cell lines. Therefore, in this study, several different cell types were used to assess specific phagocyte functions. To study the role of the protein corona, in addition to uncoated particles, also plasma-coated CPS particles were tested. The different exposure conditions limit inter-assay comparisons and physicochemical characterisation of uncoated and plasma coating was used to identify the effect of the coating on size and surface charge.

Although charge densities of the particles (indicated by the producer) increased markedly from 20 to ≥200 nm CPS particles, the zeta potential as relevant parameter for the interaction with cells, decreased from 20 to 1,000 nm CPS, in both uncoated and plasma-coated particles. Polystyrene particles show a high tendency to agglomerate, for instance in medium +10 %

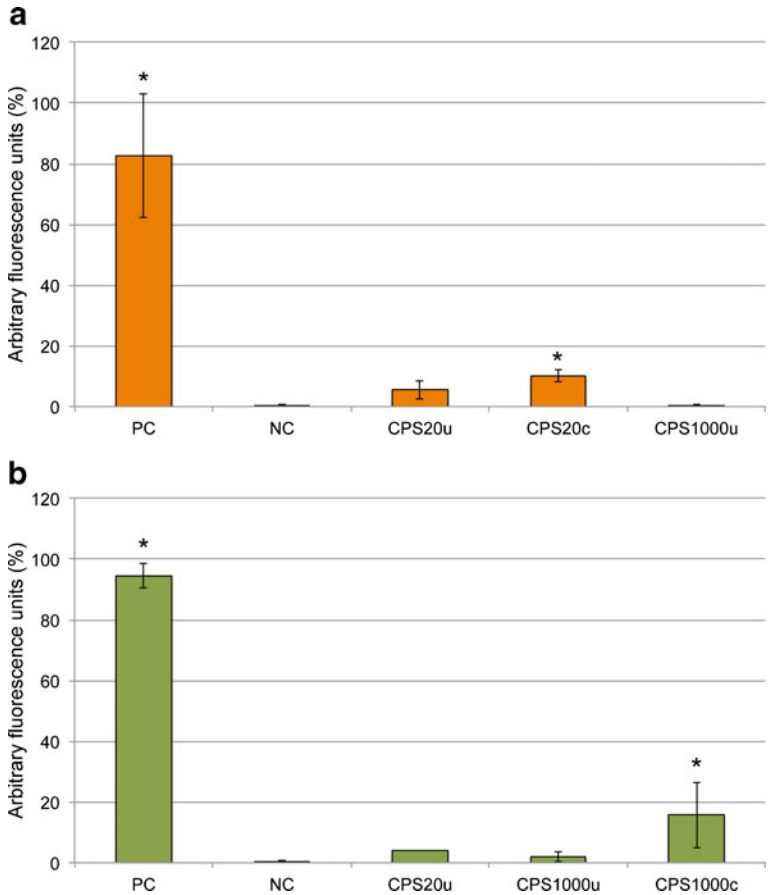

Fig. 7 Generation of superoxide in monocytes (**a**) and granulocytes (**b**) in human blood samples exposed to 25 μg/ml CPS particles suspended in PBS (n=4). *E. coli* provided in the assay kit served as positive control (*PC*) and PBS as negative control (*NC*). Data are normalised to the generation of superoxide in cells exposed to buffer. **a** Uncoated and plasma-coated 20 nm CPS particles increase the production of superoxide by monocytes while 1,000 nm CPS particles display only a marginal effect. **b** In granulocytes, plasma-coated 1,000 nm CPS particles increase the production of superoxide while 20 nm CPS particles display only a marginal effect. Significant changes to the solvent-treated controls (p<0.05) are indicated by *asterisk*. *u* uncoated, *c* plasma coated

FBS. These larger particles are no more cytotoxic (Fröhlich et al. 2009). Particles were, therefore, coated to mimic the physiological situation, namely the formation of a protein corona (Lundqvist et al. 2008), while preventing size increases observed in medium +10 % FBS.

Despite similar sizes of uncoated and plasma-coated particles, 20 nm uncoated CPS particles were taken up

Table 3 Overview of assays, cell types, concentrations, and particles and obtained effects

Assay	Cells	Concentrations (μg/ml)	Particles (sizes, nm)	Sign. effect at concentrations of ≤100 μg/ml
Viability	U937, THP-1, THPdiff, DMBM-2	25-50-100-200-400-500	20-100-500-1,000	THPdiff 20, U937 20, THP 20, THPdiff 500, decrease
Chemotaxis (pre-incubation)	U937	10-50	20-200-1,000	CPS1000, increase
Cytokine release IL-6/IL-8	THP-1, THP-1diff, U937, DMBM-2	10-20-50	20-100-200-500-1,000	IL-6: THPdiff 500, THPdiff 1000; IL-8: THPdiff 20, THPdiff 500, THP 20, increase
Phagocytosis	DMBM-2	10-50 (only CPS20) 100-500	20-200-500-1,000	CPS500, CPS1000, increase
Nitric oxide generation	DMBM-2	50-100-200-500-1,000	20-200-500-1,000	None
Oxidative burst	Granulocytes, monocytes	25-50-100	20-1,000	CPS1000c granulos, CPS20c monos, increase
Myeloperoxidase	Granulocytes	50-200-2,000	20-200-500	None

to a higher degree than the plasma-coated particles. Protein coating of nanoparticles may prevent interaction of nanoparticles with plasma membranes by reduction of surface reactivity. Lack of protein coating with subsequent membrane damage could also explain energy-independent uptake of 20 nm CPS particles observed in this study. Uptake experiments were performed using incubation of peripheral blood monocytic cells with 25 μg/ml CPS particles. Significant decrease in viability after 24 h of exposure to 20 nm CPS particles showed inter-donor variations and were observed at concentrations of 100–500 μg/ml. Since non-cytotoxic concentrations were used for the uptake study, it appears less likely that membrane damage could explain the energy-independent uptake. Mechanisms different from phagocytosis and endocytosis could be involved in this energy-independent uptake (Rothen-Rutishauser et al. 2006). Variety of the composition and the rapid exchange of proteins bound to the particle (Tenzer et al. 2013) also raises the question to which extent the particles used in this study were covered by plasma proteins. On the other hand, an increased uptake of plasma-coated ≥500 nm CPS particles compared to the non-plasma-coated ones was seen in this study. This trend is opposite to the observed decrease in particle uptake of plasma-coated 20 nm CPS particles and can be explained by binding of plasma proteins (opsonisation) and receptor-mediated uptake by phagocytes in combination with unspecific adherence of phagocytes to surface-absorbed serum proteins facilitating phagocytosis (Nie 2010).

Cytotoxicity was assessed in protein-free medium to avoid agglomeration of CPS particles. Phagocytes grown in suspension (monocytes) were more sensitive to the cytotoxic action of 20 nm CPS particles than the adherent DMBM-2 cells. This higher sensitivity of adherent cells compared to cells growing in suspension is consistent with previous studies (Fröhlich et al. 2012b), where estimated IC_{50} values for 20 nm CPS particles were 182±98 μg/ml in adherent cell lines and 33± 10 μg/ml in suspension cells. The higher sensitivity is not due to an increased uptake of these particles because THP-1 monocytes ingested almost 100 times less CPS particles than DMBM-2 macrophages (Table 2 and Table 2s). It is more likely that the greater membrane surface area of suspension cells exposed to the reactive nanoparticle surface is responsible for the increased cytotoxicity (Fig. 3). A stronger disruptive effect on plasma membrane can be explained by the fact that the membrane area available for particle contact in suspension cells is larger than for adherent cells, where particles cannot get access to the part of the cell adhering to the plate. It has been hypothesised that the higher cytotoxicity of particles in protein-free media is caused by the higher surface energies in the absence of protein (Lesniak et al. 2012). Thus, in itself size is not necessarily the only parameter to be taken into account when one observes biological consequences (Lesniak et al. 2013). The higher cytotoxicity of ≥500 nm CPS particles to macrophages suggests that their toxicity may be linked to phagocytosis. This effect, however, was observed only at high particle concentrations, rendering its physiological relevance questionable.

Cytokine secretion was also assessed in the protein-free medium. IL-6 secretion increased with particle size, while IL-8 secretion showed the opposite trend in THP-1 monocytes. Changes were observed after exposure to a concentration of 20 μg/ml particles, where release of interleukins due to membrane damage by 20 nm CPS particles cannot be excluded. Cytokine releases obtained by incubation with 10 μg/ml 20 nm CPS, however, were almost identical to secretions obtained by incubation with the potentially cytotoxic concentrations. This could be due to the fact that polystyrene particles can bind proteins and binding to more particles could decrease measured interleukin levels. On the other hand, interleukin levels might not be increased in cells with decreased viability because the compromised cells did not produce interleukin. Increases in interleukin secretion induced by micro- and nano-sized CPS particles were of a similar order of magnitude. For carbon black particles and silica particles, particle size was inversely correlated with cytokine secretion: small, 14 nm carbon black particles produced higher increases in cytokine levels than 95 nm particles (Shwe et al. 2005); 70 nm silica NPs induced cytokine release but 300 and 1,000 nm particles did not (Nishimori et al. 2009) and 50 nm silica NPs had a more potent effect on IL-1β release than the 500 nm particles (Sandberg et al. 2012). The higher reactivity of the nano-sized particles may be due to the generation of reactive oxygen species, which has been reported for these materials but only occurs to a small extent in CPS particles (Fröhlich et al. 2009). In contrast to the reaction to carbon black and silica particles, cytokine release from macrophages was higher for 0.5 and 4.3 μm ceramic particles than for 0.2 and 7.2 μm particles (Catelas et al. 1998). The finding that 500 nm and 1000 nm CPS particles in this study significantly

increased phagocytosis, suggests that the release of inflammatory cytokines by microparticles may be linked to phagocytosis.

Reported effects of ultrafine particles and carbon black and of micro-sized cobalt-chrome wear and poly(lactic *co*-glycolic acid) particles on phagocytosis are predominantly inhibitory (Garrett et al. 1983; Renwick et al. 2001; Jones et al. 2002; Bernard et al. 2007). In contrast to that, significant increases in phagocytosis of *E. coli* indicator particles induced by rather high concentrations of 500 and 1,000 nm CPS particles were identified in this study. Since increases in phagocytosis induced by these particles at lower concentrations were smaller, a contribution of cell damage to the observed effect cannot be excluded.

In this study, 20 nm CPS particles displayed no effect, while large CPS particles increased chemotaxis. Nano-sized superparamagnetic iron nanoparticles showed no effect on chemotaxis (Walter et al. 2008), whereas carbon nanotubes, polymethylmethacrylate NPs, and TiO_2 NPs, suppressed chemotaxis (Papatheofanis and Barmada 1991; Witasp et al. 2009; Liu et al. 2010). Since cytotoxicity and interaction with the cytoskeleton (carbon nanotubes) were not excluded in these studies, inhibition of chemotaxis might be a manifestation of cytotoxicity. Activation of chemotaxis by 1,000 nm CPS particles is similar to increased chemotaxis caused by polyethylene microparticles in vivo (Frokjaer et al. 1995).

While TiO_2, Ti and V nanoparticles and polyethylene wear particles increased superoxide production in granulocytes (Hedenborg 1988; Kumazawa et al. 2002; Bernard et al. 2007; Jovanovic et al. 2011), only the larger CPS particles showed this effect in this study. The absence of stimulation by the 20 nm CPS particles in this study could be explained by the absence of metal ions and endotoxin, which could be involved in the effect caused by TiO_2, Ti and V NPs.

Some effects, namely generation of nitric oxide and degranulation of granulocytes were only detected at high, not physiologically relevant concentrations. Generation of nitric oxide has been reported for pegylated gold NPs, silica NPs and TiO_2 NPs (Park and Park 2009; Hutter et al. 2010; Scherbart et al. 2011). Lack of influence on granulocyte degranulation has been reported for TiO_2 NPs (Jovanovic et al. 2011; Vesnina et al. 2011).

The presented data suggest that cytotoxicity of 20 nm CPS particles might be caused by ingestion of a higher number of particles with concomitant plasma membrane damage. Membrane damage could also be involved in increased interleukin secretion or oxidative burst in monocytes. Although 100 nm CPS particles are taken up in higher numbers than 500 and 1,000 nm CPS particles, their cytotoxicity was much lower. While the larger CPS particles induced oxidative burst with ROS generation and cell damage, CPS particles in the size range between 20 and 500 nm were taken up without obvious interference with cell viability and function. At non-cytotoxic concentrations, it appears that micro-sized CPS particles show stronger interference with phagocyte function (chemotaxis, interleukin secretion, phagocytosis and oxidative burst of granulocytes) than nano-sized CPS particles.

Acknowledgments The authors thank Diana Mujk and Nicole Muhry (ELISA), Tatjana Kueznik and Markus Absenger (microscopy) and Evelyne Höller (immune assays) for excellent technical assistance, and Alison Green for help with the manuscript. This work was supported by the FP6 European integrated project "NanoBiopharmaceutics", NMP4-CT-2006-026723, the Austrian Science Fund grants N 214-NAN and P22576-B18 and the Research and Technology Development in Project Cluster NANO-HEALTH.

Conflicts of interest The authors declare that there are no conflicts of interest.

References

Allermann L, Poulsen OM. Interleukin-8 secretion from monocytic cell lines for evaluation of the inflammatory potential of organic dust. Environ Res. 2002;88:188–98.

Bernard L, Vaudaux P, Huggler E, Stern R, Frehel C, Francois P, et al. Inactivation of a subpopulation of human neutrophils by exposure to ultrahigh-molecular-weight polyethylene wear debris. FEMS Immunol Med Microbiol. 2007;49:425–32.

Catelas I, Huk OL, Petit A, Zukor DJ, Marchand R, Yahia L. Flow cytometric analysis of macrophage response to ceramic and polyethylene particles: effects of size, concentration, and composition. J Biomed Mater Res. 1998;41:600–7.

Champion JA, Mitragotri S. Shape induced inhibition of phagocytosis of polymer particles. Pharm Res. 2009;26:244–9.

Fröhlich E, Samberger C, Kueznik T, Absenger M, Roblegg E, Zimmer A, et al. Cytotoxicity of nanoparticles independent from oxidative stress. J Toxicol Sci. 2009;34:363–75.

Fröhlich E, Meindl C, Roblegg E, Ebner B, Absenger M, Pieber TR. Action of polystyrene nanoparticles of different sizes on lysosomal function and integrity. Part Fibre Toxicol. 2012a;9:26.

Fröhlich E, Meindl C, Roblegg E, Griesbacher A, Pieber TR. Cytotoxicity of nanoparticles is influenced by size, proliferation and embryonic origin of the cells used for testing. Nanotoxicology. 2012b;6:424–3.

Fröhlich E, Bonstingl G, Hofler A, Meindl C, Leitinger G, Pieber TR, et al. Comparison of two in vitro systems to assess

cellular effects of nanoparticles-containing aerosols. Toxicol in vitro. 2013;27:409–17.
Frokjaer J, Deleuran B, Lind M, Overgaard S, Soballe K, Bunger C. Polyethylene particles stimulate monocyte chemotactic and activating factor production in synovial mononuclear cells in vivo. An immunohistochemical study in rabbits. Acta Orthop Scand. 1995;66:303–7.
Garrett R, Wilksch J, Vernon-Roberts B. Effects of cobalt-chrome alloy wear particles on the morphology, viability and phagocytic activity of murine macrophages in vitro. Aust J Exp Biol Med Sci. 1983;61(Pt 3):355–69.
Gosens I, Post JA, de la Fonteyne LJ, Jansen EH, Geus JW, Cassee FR, et al. Impact of agglomeration state of nano- and submicron sized gold particles on pulmonary inflammation. Part Fibre Toxicol. 2010;7:37.
Hedenborg M. Titanium dioxide induced chemiluminescence of human polymorphonuclear leukocytes. Int Arch Occup Environ Health. 1988;61:1–6.
Heng BC, Zhao X, Tan EC, Khamis N, Assodani A, Xiong S, et al. Evaluation of the cytotoxic and inflammatory potential of differentially shaped zinc oxide nanoparticles. Arch Toxicol. 2011;85:1517–28.
Hirst SM, Karakoti AS, Tyler RD, Sriranganathan N, Seal S, Reilly CM. Anti-inflammatory properties of cerium oxide nanoparticles. Small. 2009;5:2848–56.
Hsiao JK, Chu HH, Wang YH, Lai CW, Chou PT, Hsieh ST, et al. Macrophage physiological function after superparamagnetic iron oxide labeling. NMR Biomed. 2008;21:820–9.
Hutter E, Boridy S, Labrecque S, Lalancette-Hebert M, Kriz J, Winnik FM, et al. Microglial response to gold nanoparticles. ACS nano. 2010;4:2595–606.
Inoue K, Takano H, Yanagisawa R, Koike E, Shimada A. Size effects of latex nanomaterials on lung inflammation in mice. Toxicol Appl Pharmacol. 2009;234:68–76.
Jones BG, Dickinson PA, Gumbleton M, Kellaway IW. The inhibition of phagocytosis of respirable microspheres by alveolar and peritoneal macrophages. Int J Pharm. 2002;236:65–79.
Jovanovic B, Anastasova L, Rowe EW, Zhang Y, Clapp AR, Palic D. Effects of nanosized titanium dioxide on innate immune system of fathead minnow (*Pimephales promelas* Rafinesque, 1820). Ecotoxicol Environ Saf. 2011;74:675–83.
Kumazawa R, Watari F, Takashi N, Tanimura Y, Uo M, Totsuka Y. Effects of Ti ions and particles on neutrophil function and morphology. Biomaterials. 2002;23:3757–64.
Lesniak A, Fenaroli F, Monopoli MP, Aberg C, Dawson KA, Salvati A. Effects of the presence or absence of a protein corona on silica nanoparticle uptake and impact on cells. ACS nano. 2012;6:5845–57.
Lesniak A, Salvati A, Santos-Martinez MJ, Radomski MW, Dawson KA, Aberg C. Nanoparticle adhesion to the cell membrane and its effect on nanoparticle uptake efficiency. J Am Chem Soc. 2013;135:1438–44.
Liu R, Yin LH, Pu YP, Li YH, Zhang XQ, Liang GY, et al. The immune toxicity of titanium dioxide on primary pulmonary alveolar macrophages relies on their surface area and crystal structure. J Nanosci Nanotechnol. 2010;10:8491–9.
Lundqvist M, Stigler J, Elia G, Lynch I, Cedervall T, Dawson KA. Nanoparticle size and surface properties determine the protein corona with possible implications for biological impacts. Proc Natl Acad Sci U S A. 2008;105:14265–70.
Mainardes RM, Gremiao MP, Brunetti IL, da Fonseca LM, Khalil NM. Zidovudine-loaded PLA and PLA-PEG blend nanoparticles: influence of polymer type on phagocytic uptake by polymorphonuclear cells. J Pharm Sci. 2009;98:257–67.
Nie S. Understanding and overcoming major barriers in cancer nanomedicine. Nanomedicine: Nanotech Biol Med. 2010;5:523–8.
Nishimori H, Kondoh M, Isoda K, Tsunoda S, Tsutsumi Y, Yagi K. Silica nanoparticles as hepatotoxicants. Eur J Pharm Biopharm. 2009;72:496–501.
Olivier V, Duval JL, Hindie M, Pouletaut P, Nagel MD. Comparative particle-induced cytotoxicity toward macrophages and fibroblasts. Cell Biol Toxicol. 2003;19:145–59.
Papatheofanis FJ, Barmada R. Polymorphonuclear leukocyte degranulation with exposure to polymethylmethacrylate nanoparticles. J Biomed Mater Res. 1991;25:761–71.
Park EJ, Park K. Oxidative stress and pro-inflammatory responses induced by silica nanoparticles in vivo and in vitro. Toxicol Lett. 2009;184:18–25.
Renwick LC, Donaldson K, Clouter A. Impairment of alveolar macrophage phagocytosis by ultrafine particles. Toxicol Appl Pharmacol. 2001;172:119–27.
Roblegg E, Fröhlich E, Meindl C, Teubl B, Zaversky M, Zimmer A. Evaluation of a physiological in vitro system to study the transport of nanoparticles through the buccal mucosa. Nanotoxicology. 2012;6:399–413.
Rothen-Rutishauser BM, Schurch S, Haenni B, Kapp N, Gehr P. Interaction of fine particles and nanoparticles with red blood cells visualized with advanced microscopic techniques. Environ Sci Technol. 2006;40:4353–9.
Sandberg W, Låg M, Holme J, Friede B, Gualtieri M, Kruszewski M, et al. Comparison of non-crystalline silica nanoparticles in IL-1ß release from macrophages. Part Fibre Toxicol. 2012;9:32.
Scheel J, Weimans S, Thiemann A, Heisler E, Hermann M. Exposure of the murine RAW 264.7 macrophage cell line to hydroxyapatite dispersions of various composition and morphology: assessment of cytotoxicity, activation and stress response. Toxicol in vitro. 2009;23:531–8.
Scherbart AM, Langer J, Bushmelev A, van Berlo D, Haberzettl P, van Schooten FJ, et al. Contrasting macrophage activation by fine and ultrafine titanium dioxide particles is associated with different uptake mechanisms. Part Fibre Toxicol. 2011;8:31.
Segat D, Tavano R, Donini M, Selvestrel F, Rio-Echevarria I, Rojnik M, et al. Proinflammatory effects of bare and PEGylated ORMOSIL-, PLGA- and SUV-NPs on monocytes and PMNs and their modulation by f-MLP. Nanomedicine: Nanotech Biol Med. 2011;6:1027–46.
Shavandi Z, Ghazanfari T, Moghaddam KN. In vitro toxicity of silver nanoparticles on murine peritoneal macrophages. Immunopharmacol Immunotoxicol. 2011;33:135–40.
Shwe TT, Yamamoto S, Kakeyama M, Kobayashi T, Fujimaki H. Effect of intratracheal instillation of ultrafine carbon black on proinflammatory cytokine and chemokine release and mRNA expression in lung and lymph nodes of mice. Toxicol Appl Pharmacol. 2005;209:51–61.
Tenzer S, Docter D, Kuharev J, Musyanovych A, Fetz V, Hecht R, et al. Rapid formation of plasma protein corona critically affects nanoparticle pathophysiology. Nat Nanotechnol. 2013;8:772–81.

Vesnina LE, Mamontova TV, Mikitiuk MV, Kutsenko NL, Kutsenko LA, Bobrova NA, et al. Effect of fullerene C60 on functional activity of phagocytic cells. Eksp Klin Farmakol. 2011;74:26–9.

Villiers C, Freitas H, Couderc R, Villiers MB, Marche P. Analysis of the toxicity of gold nano particles on the immune system: effect on dendritic cell functions. J Nanopart Res. 2010;12: 55–60.

Walter G, Santra S, Thattaliyath B, Grant S. (Super)paramagnetic nanoparticles: applications in noninvasive MR imaging of stem cell transfer. In: Bulte J, Modo M, editors. Fundamental biomedical technologies nanoparticles in biomedical imaging emerging technologies and applications. New York: Springer; 2008.

Winter M, Beer HD, Hornung V, Kramer U, Schins RP, Forster I. Activation of the inflammasome by amorphous silica and TiO_2 nanoparticles in murine dendritic cells. Nanotoxicology. 2011;5:326–40.

Witasp E, Shvedova AA, Kagan VE, Fadeel B. Single-walled carbon nanotubes impair human macrophage engulfment of apoptotic cell corpses. Inhal Toxicol. 2009;21 Suppl 1:131–6.

Yang EJ, Kim S, Kim JS, Choi IH. Inflammasome formation and IL-1beta release by human blood monocytes in response to silver nanoparticles. Biomaterials. 2012;33:6858–67.

Yue H, Wei W, Yue Z, Lv P, Wang L, Ma G, et al. Particle size affects the cellular response in macrophages. Eur J Pharm Sci. 2010;41:650–7.